

## Magnetic Field Line Escape: Comparison with Mean Free Path

This content has been downloaded from IOPscience. Please scroll down to see the full text.

2011 J. Phys.: Conf. Ser. 285 012012

(<http://iopscience.iop.org/1742-6596/285/1/012012>)

View [the table of contents for this issue](#), or go to the [journal homepage](#) for more

Download details:

IP Address: 143.107.134.77

This content was downloaded on 30/01/2015 at 11:22

Please note that [terms and conditions apply](#).

# Magnetic Field Line Escape: Comparison with Mean Free Path

Caroline G. L. Martins<sup>1,2</sup>, M. Roberto<sup>2</sup>, I. L. Caldas<sup>3</sup> and R. Egydio de Carvalho<sup>1</sup>

<sup>1</sup> UNESP-Univ Estadual Paulista; Instituto de Geociências e Ciências Exatas; Departamento de Estatística, Matemática Aplicada e Computação, Av. 24A, 1515, 13506-900 Rio Claro, SP, Brazil.

<sup>2</sup> Instituto Tecnológico da Aeronáutica; Departamento de Física 12228-900 São José dos Campos, SP, Brazil.

<sup>3</sup> Universidade de São Paulo; Instituto de Física 05315-970 São Paulo, SP, Brazil.

E-mails: carolinegameiro@gmail.com, marisar@ita.br, ibere@if.usp.br and regydio@rc.unesp.br

**Abstract** In the present work, we determine the fraction of magnetic field lines that reach the tokamak wall leaving the plasma surrounded by a chaotic layer created by resonant perturbations at the plasma edge. The chaotic layer arises in a scenario where an integrable magnetic field with reversed magnetic shear is perturbed by an ergodic magnetic limiter. For each considered line, we calculate its connection length, i.e. the number of toroidal turns that the field lines complete before reaching the wall. We represent the results in the poloidal section in which the initial coordinates are chosen. We also estimate the radial profile of the fraction of field lines, for different temperatures, whose connection lengths are smaller than the electron collisional mean free path.

## 1. Introduction

Plasma-wall interaction is one of the critical issues for the development of an energy source based on nuclear fusion [1-3]. Efforts have been made to study particle transport in tokamaks outer of the plasma column to verify how this transport affects the tokamak wall. If the heat and particle loadings are too spatially localized, the sputtering processes which occur in the wall may release contaminants into the plasma column deteriorating the overall confinement quality [4].

Many techniques have been developed to modify the spatial distribution of the particles and of the heat transport in the outer region of the tokamak in order to improve the plasma confinement. One of these techniques uses an ergodic magnetic limiter that creates resonant magnetic perturbations at the plasma edge and generates a chaotic layer near the tokamak wall [5-7].

Another way to improve the confinement is to modify the plasma current to create an equilibrium with reversed magnetic shear from a non-monotonic plasma current density. In this case an internal barrier arises and the particle transport is reduced [8, 9].

A recent work has shown that the connection lengths are comparable to the electron collisional mean free path for tokamaks with divertors [10]. In our work, we are going to study the patterns produced by the escaping chaotic field line near the tokamak wall [11, 12] for an equilibrium with reversed magnetic shear perturbed by an ergodic magnetic limiter. The escaping of the field line is analyzed for a range of control parameters and the connections lengths are calculated and compared to

the electron collisional mean free path in order to estimate the relevance of the field line transport. The comparison is made for different radial positions and different temperature values.

## 2. Hamiltonian Approach

In this section we introduce a Hamiltonian to describe the plasma equilibrium with a reversed shear magnetic field in the tokamak perturbed by an ergodic magnetic limiter (EML). The equilibrium Hamiltonian,  $H_0$ , has a toroidal symmetry whose canonical time is the associated toroidal angle  $\phi$  (See Figure 1). This integrable non-perturbed Hamiltonian corresponds to an analytical solution of the non-linear Grad-Shafranov equation [13].

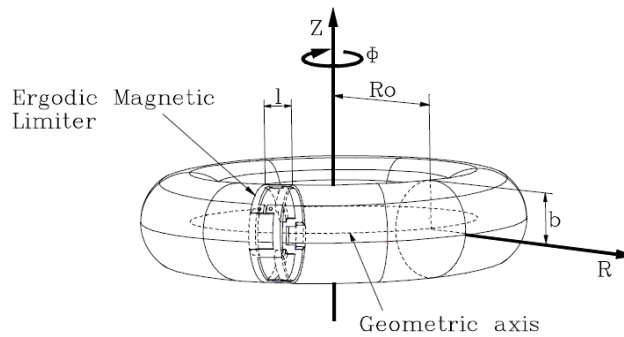


**Figure.1** - Basic geometry of the tokamak with the ergodic magnetic limiter scheme.

The field lines geometry is described in non-orthogonal polar-toroidal coordinates  $(r_p, \theta_p, \phi_t)$  [13], which are related to the polar local coordinates  $(r, \theta)$  by this relation:

$$r_t = r \left[ 1 - \frac{r}{R_0'} \cos \theta + \left( \frac{r}{2R_0'} \right)^2 \right]^{1/2} \quad \text{and} \quad \sin \theta_t = \sin \theta \left[ 1 - \frac{r}{R_0'} \cos \theta + \left( \frac{r}{2R_0'} \right)^2 \right]^{-1/2} \quad (1)$$

where  $R_0'$  is the Shafranov shift. This coordinate system has been introduced to evidence the toroidal effects in the geometry of equilibrium field. Magnetic surfaces are characterized by nested surfaces of  $r_t = \text{constant}$ , for which the non-monotonic safety factor [14] reads as,

$$q_c(r_t) = q_c(a) \frac{r_t^2}{r^a} \left[ 1 - \left( 1 + \beta' \left( \frac{rt}{a} \right)^2 \right) \left( 1 - \left( \frac{rt}{a} \right)^2 \right)^{\gamma+1} \right]^{-1} \quad (2)$$

with  $q_c(a) = (I_p a^2)/(I_e R_0^2)$ , where  $I_p$  is the total plasma current,  $I_e$  is the total current of the toroidal magnetic system,  $a$  is the plasma radius,  $R_0$  is the position of the magnetic axis and the parameters  $\gamma=0.78$  and  $\beta=3.0$ , with  $\beta' = \beta(\gamma+1)/(\beta+\gamma+2)$ , describes the plasma current profile.

We have chosen  $q \approx 5$  at the plasma edge with  $R_0=0.61$  m and  $a=0.18$  m, which are the TCABR parameters [15].  $R_0$  is the major radius and  $a$  is the plasma radius.

The perturbing Hamiltonian  $H_t$  is created by an ergodic magnetic limiter that consists of  $N_r$  rings of length  $l$  located symmetrically along the toroidal direction of the tokamak (see Figure 1). These current rings may be considered as slices of a pair of external helical windings located at  $r_t = b$ , which conduct a current  $I_h$  in opposite senses for adjacent conductors. The windings are described by the following winding law:  $u_t = m_0[\theta_t + a \sin(\theta_t)] - n_0 \phi_t$ , where  $(m_0, n_0)$  are the poloidal and toroidal mode numbers, respectively [14]. A tunable parameter  $\alpha$  is introduced in such way that the variable  $u_t$  is constant along a field line.

After an appropriated canonical transformation, the unperturbed Hamiltonian  $H_0$  is given in terms of the action  $J$ , corresponding to the toroidal normalized flux, and  $\vartheta$  the poloidal angle canonically associated to  $J$ . The perturbing Hamiltonian  $H_1$  is a function of  $J$ ,  $\vartheta$  and  $t$ , and it is represented by a Fourier expansion of delta-kicks due to the ergodic magnetic limiter [14]. The perturbation creates chaotic magnetic field lines at the plasma edge, and the Hamiltonian function that describes the perturbed magnetic field lines is:

$$H(J, \vartheta, t) = H_0(J) + \varepsilon \sum_{m=0}^{2m_0} H_m^*(J) \cos(m\vartheta - nt) \sum_{k=-\infty}^{+\infty} \delta\left(t - \frac{2\pi}{N_r} k\right) \quad (3)$$

where  $H_m^*$  are the Fourier coefficients and the perturbation strength is given by,

$$\varepsilon = -2 \left( \frac{l}{2\pi R_0} \right) \left( \frac{I_h}{I_e} \right) \quad (4)$$

The value of epsilon is very small because in tokamaks we have  $l \ll 2\pi R_0$  and  $I_h \ll I_e$ . The details of this derivation can be found in [14].

### 3. Connection Lengths

For a magnetic field line with an initial position given by  $(J, \vartheta)$  in the considered Poincaré section ( $\Phi = 0$ ), its connection length  $N_{cl}(J, \vartheta)$  is the number of toroidal turns completed before the lines reaches the tokamak wall. In our case we can coincide the ergodic limiter with the tokamak wall at the same radius, for instance  $r_t = b$  (corresponding to  $J=0.055$ ). The field line is considered lost when it reaches this radial position. The non-uniformity at the plasma edge, due to chaos, can be described by the field line connection length distribution.

Figure 2(a) shows the distribution of the connection length values  $N_{cl}(J, \vartheta)$  numerically calculated for a grid of 200 x 1000 initial conditions of  $(J, \vartheta)$ . The color scale in the figure indicates the  $N_{cl}$  values from 1 to 500 toroidal turns. In this figure, the lines trapped inside the islands are represented by pink points. We consider the perturbation parameter  $I_h/I_p=0.11$ , and the perturbation mode number as  $(m_0, n_0) = (4, 1)$ . In Figure 2(a) initial conditions with different colors indicate that the field lines with large and small connection lengths are densely mixed, as found in reference [12]. Figure 2(b) shows the fraction of lines that escape toward the wall, as a function of the initial position  $J$ , relative to the total number of field lines lost to the wall.

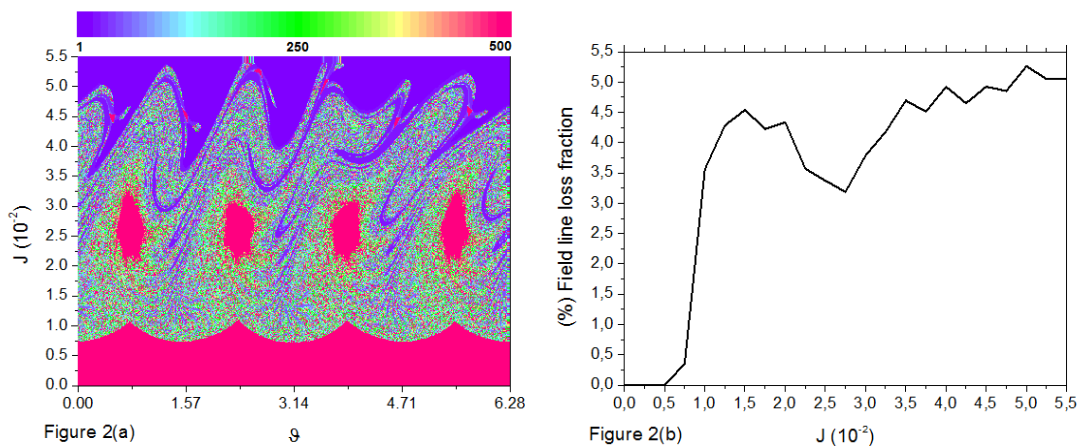


**Figure 2 - (a)** Connection lengths for  $q(a)=5$ . Scale from 1 to 500 toroidal turns. **(b)** Percentage of lines that escape toward the wall.

As we can see in Figs. 2(a) and 2(b), the escaping of the field lines is higher at the tokamak edge than in the plasma core. We also note the existence of four islands of stability (four elliptic fixed points) at the position  $J \approx 0.025$ . This fact leads to the decreasing of the field lines loss to the wall, because of the stickiness around the magnetic islands, which traps the magnetic field lines and increases their connection lengths. Moreover, these islands are surviving dimerized islands typical of plasma equilibrium with a non-monotonic spatial safety factor profile as the one considered in this work.

#### 4. Comparisons Between Mean Free Path (MFP) and Connection Lengths

The electron mean free path  $\lambda$  can be estimated by the formula [16]

$$\lambda = 2.5 \times 10^{17} \frac{T_e^2}{n_e \ln(\Lambda)} \quad (5)$$

where the temperature is in eV and the density is in  $\text{m}^{-3}$ . To obtain  $\lambda$  in Eq. (5), we use the plasma density  $n_e = 5.0 \times 10^{18} \text{ (m}^{-3}\text{)}$ ,  $\ln(\Lambda) = 15.2 - 0.5 \ln(n_e/10^{20}) + \ln(T_e/1000)$  and different values of electron temperature  $T_e$ . Table 1 presents the values obtained for  $\lambda$ , considering temperatures from 10 to 100 eV. The ratio  $\lambda/2\pi R_0$  is equivalent to the mean free path in units of toroidal length and  $2\pi R_0$  is the toroidal circumference length.

<b><math>T_e</math> (eV)</b>	<b><math>\lambda</math> (m)</b>	<b><math>(\lambda/2\pi R_0)</math></b>
10	0,4137	0,1078
20	1,5642	0,4081
30	3,4113	0,8900
40	5,9351	1,5485
50	9,1226	2,3801
60	12,9641	3,3824
70	17,4518	4,5533
80	22,5795	5,8912
90	28,3416	7,3946
100	34,7336	9,0623

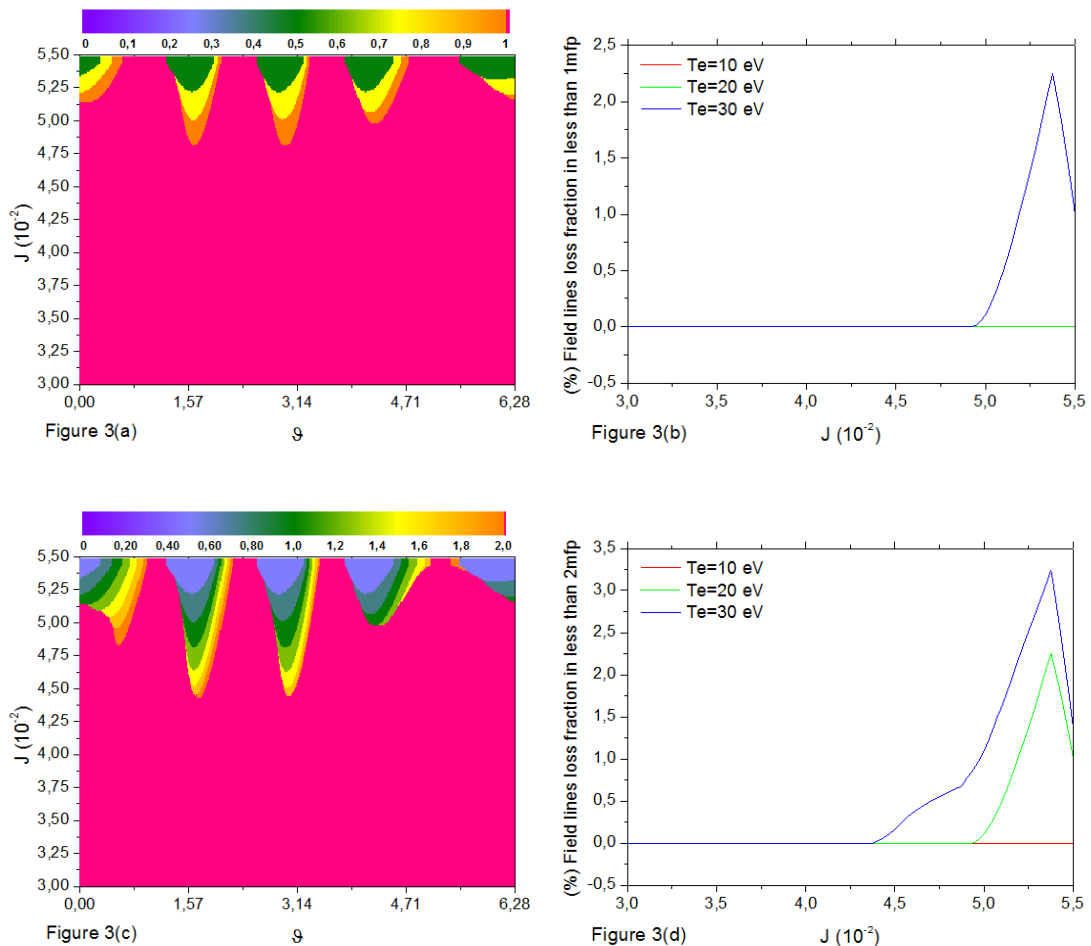
**Table 1** – Mean free paths ( $\lambda$ ) and the ratio ( $\lambda/2\pi R_0$ ), from  $T_e=10$  to  $T_e=100$  eV.

Figure 3 shows the calculated connection lengths for the field lines with initial coordinates  $(J, \vartheta)$ . The actions are in the interval  $J = [0,030; 0,055]$  and the scale represent values from 0 to  $\lambda$  (fig. 3a) and from 0 to  $2\lambda$  (fig. 3c). In Figs. 3b and 3d we also present the action profiles of the fraction of lines lost with connection lengths smaller than  $\lambda$  (in fig. 3b) and  $2\lambda$  (in fig. 3d).

Close to the plasma edge, the field lines have smaller connection lengths than in the plasma core, as one can verify in Figs. 2 and 3. The reason for this behavior is the existence of magnetic islands showed in Figure 2(a) (pink circles surrounded by colorful structures). These islands create a chaotic region with stickiness in their neighborhood trapping the magnetic field lines and, consequently, increasing the number of toroidal turns they complete before reaching the wall, i.e., increasing the connection lengths in the region [12]. As we are interested in the peripheral region of the plasma, we choose the range  $J = [0,030; 0,055]$ , which corresponds to the plasma edge.

Near the wall there are purple regions in Figure 2(a) corresponding to field lines with low connection lengths, which are comparable to the mean free paths analyzed above. In order to make visible the structures in the distributions, we adjusted the connection length scales,  $N_{cl}$ , varying from 0 to 1 and  $N_{cl}$  from 0 to 2, as we can see in Figs. 3(a) and 3(c), respectively. Figure 3(b) shows that the number of the field lines that escapes with less than one mean free paths increases for larger values of  $J$ . In figure 3(d) we present the same analysis but for two mean free paths. The mean free path increases with the temperature, therefore the fraction of lost field lines in such displacement also

increases. Looking at Figs. 3(b) and 3(d) we see that the percentage of lost field lines, with connection length shorter than one and two mean free paths respectively, corresponds to a maximum around 3,5% of the whole field lines that escape to the wall.



**Figure 3** - (a) Connection lengths for  $q(a)=5$  and a scale with colors indicating  $N_{cl}$  from 0 to 1. (b) Percentage of lost field lines with  $N_{cl} < \lambda$ . (c) Connection length with  $q(a)=5$  and a scale with colors indicating  $N_{cl}$  from 0 to 2 (d) Percentage of lost field lines with  $N_{cl} < 2\lambda$ .

Figures 4(a) and 4(c) show the field lines that are lost during a displacement of less than one and two collisional mean free paths respectively, as a function of the variable action  $J$ , for electron temperatures from 40 to 100 eV.

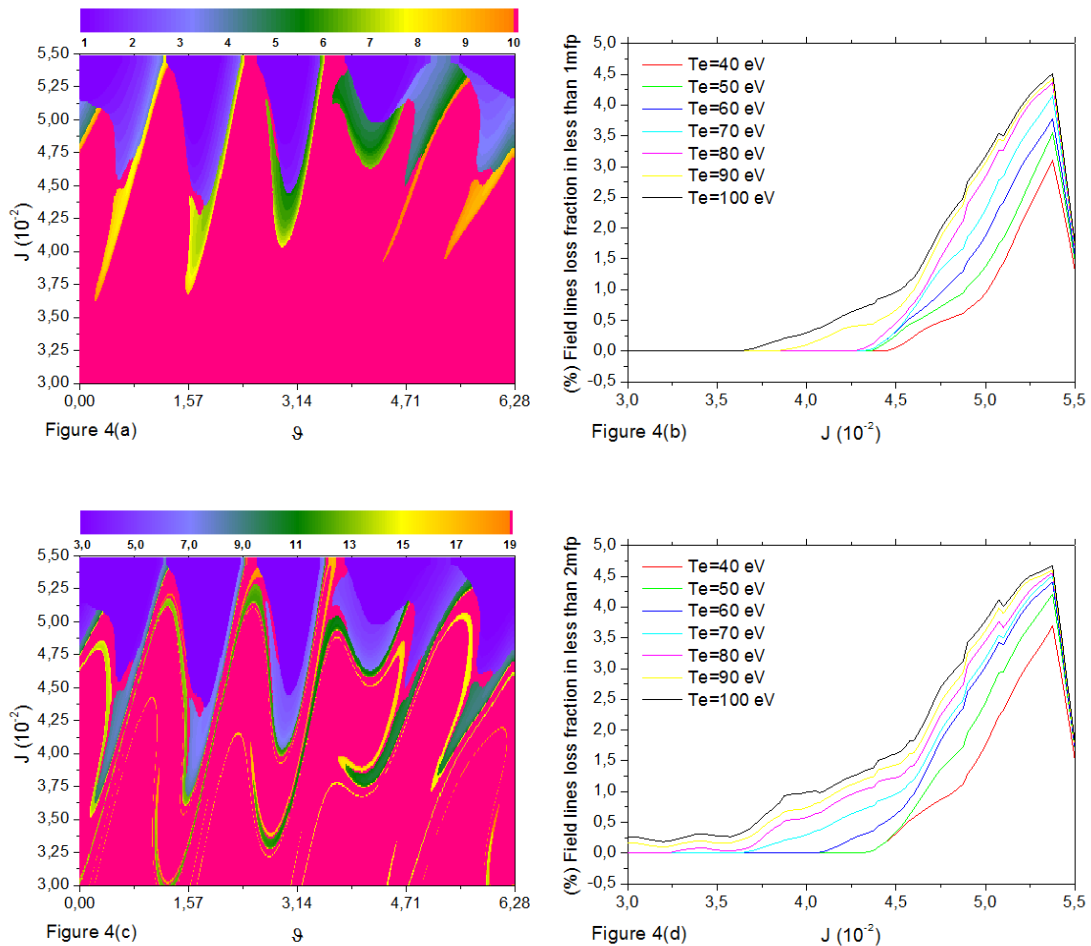


**Figure 4** - (a) Connection lengths for  $q(a)=5$ . The scale indicates colors representing  $N_{cl}$  from 1 to 10. (b) Percentage of lost field lines with  $N_{cl} < 1 \lambda$ . (c) Connection length with  $q(a)=5$  for  $N_{cl}$  scale from 3 to 19. (d) Percentage of field lines loss fraction in less than 2 collisional mean free paths.

In Figs. 4(a) and 4(c), we adjust the connection length scales to  $N_{cl} = 1$  until  $N_{cl} = 10$  and  $N_{cl} = 3$  until  $N_{cl} = 19$ , respectively. Figures 4(b) and 4(d) shows that the fraction of lost field lines increases with the temperature and the maximum percentage of lost field lines fraction increases for large values of  $T_e$ . Accordingly, the maximum values are 4,5% in Fig. 3(d) and 3,5% in Fig. 4(d).

## 5. Conclusions

We calculate the spatial connection length distribution for magnetic field lines in tokamaks with a reversed magnetic shear perturbed by an ergodic magnetic limiter. For this equilibrium, the stickiness around the dimerized magnetic islands traps magnetic field lines and increase their connection lengths.

We show that most of the magnetic field lines located inside the chaotic region describe long distances, which are much higher than the electron collisional mean free path, before reaching the tokamak wall. However, the fraction of the field lines lost to the wall with connection lengths shorter that the electron collisional mean free path increases with the electron temperature and also increases for large values of the action variable  $J$ . So, we expect that a significative fraction of field lines escape to the wall completing a toroidal excursion with a length shorter than the mean free path.

The comparison between the connection lengths obtained in this work and the electron mean free path indicates that the time for the escaping of the field line should be relevant to estimate the particle confinement time.

### Acknowledgments

The authors thank the Brazilian scientific agencies FAPESP, CNPq and CAPES for financial support.

### References

- [1] Hazeltine R D and Prager S C 2002 *Physics Today* **55** 7 30
- [2] Hidalgo C 2004 *Astrophysics and Space Science* **292** 681
- [3] Horton W 1999 *Reviews of Modern Physics* **71** 3 735
- [4] Parker R et al 1997 *J. Nucl. Mater* **241** 243
- [5] Ghendrih Ph, Grosman A and Capes H 1996 *Plasma Phys. Control. Fusion* **38** 1653
- [6] Silva E C, Caldas I L, Viana R L 2001 *IEEE Trans. On Plasma Science* **4** 617-631
- [7] Silva E C, Caldas I L, Viana R L, Sanjuán M A F 2002 *Phys. Plasmas* **9** 4917
- [8] Levinton F M et al 1995 *Phys. Rev. Lett.* **75** 4417
- [9] Connor J W, Fukuda T, Garbet X, Gormezano C 2004 *Nuclear Fusion* **44** R1-R49
- [10] Fenstermacher M E et al 2008 *Phys. Plasmas* **15** 056122
- [11] Silva E C, Roberto M, Portela J S E, Caldas I L, Viana R L 2006 *Nuclear Fusion* **46** S192-S198
- [12] Kroetz T, Roberto M, Silva E C, Caldas I L, Viana R L 2008 *Phys. Plasmas* **15** 092310
- [13] Kucinski M Y and Caldas I L 1987 *Z Naturforsch, A: Phys. Sci.* **42** 1124
- [14] Roberto M, Silva E C, Caldas I L and Viana R L 2004 *Phys. Plasma* **11**(1) 214
- [15] Nascimento I C et al 2007 *Nucl. Fusion* **47** 1570
- [16] Kotov V, Reiter D and Kukushkin A S 2007 *Report Julich* **4257** in [www.eirene.de](http://www.eirene.de)